FACTA UNIVERSITATIS (NIŠ)
Series: Electronics and Energetics vol. 13, No. 1, April 2000, 73–82

ADVANCES IN SPECTRAL METHODS FOR OPTOELECTRONIC DESIGN

Ana Vukovic, Steve Greedy, Phillip Sewell, Trevor M. Benson and Peter C. Kendall

Abstract. Two advances in spectral methods for the fast and accurate analysis of optical waveguides are reported. The Spectral Index method has been extended to include arbitrarily shaped rib waveguides in air. Then a Half Space Radiation Mode method is developed to calculate the facet reflectivity of 2D waveguides buried at realistic depth. Keywords: optoelectronics, rib waveguides, facet reflectivity

Key words: Optoelecronics, rib waveguides, facet reflectivity

1. Introduction

With the rapid development of modern optoelectronic circuits there is also an increased need for analysis techniques which can produce accurate and reliable results. Well proven numerical methods such as the Finite Difference (FD), Finite Element (FE) and the Beam Propagation Methods (BPM) are very popular since they are generally applicable and produce accurate (benchmark) results [1-3]. However, due to their large memory and time requirements they often fail within an iterative design environment.

On the other hand, the number of semi-analytical methods is continually increasing. The popularity of these methods stems from their simplicity, ease of implementation and efficiency, and the accuracy of the results. Low memory and time requirements, together with high accuracy, make them indispensable tools when evolving a design. Amongst the first methods developed were the Effective Index (EI) [4] and Weighted Index (WI) methods

Manuscript received March 14, 2000. A version of this paper was presented at the fourth IEEE Conference on Telecommunications in Modern Satellite, Cables and Broadcasting Services, TELSIKS'99, October 1999, Niš, Serbia.

The authors are with School of Electrical and Electronic Engineering, University of Nottingham, United Kingdown, e-mail is: av@nestor.eee.nott.ac.uk.

[5]. Both methods are approximate and efficient but fail to produce reliable results for propagation constants and field profiles when the structure is near cut-off. The Spectral Index (SI) method [6] is another well established and proven method for solving for the polarised modes of a wide range of optoelectronic structures based on rib waveguides. Recently, the SI method has been enhanced to explicitly include the singular behaviour of the principal field component in the vicinity of the re-entrant corners which provides improved accuracy in calculations of the modal propagation constant [7].

Another well proven technique for analysing optical devices is the Free Space Radiation Mode (FSRM) method, originally developed for buried waveguide analysis [8]. It has been applied to the analysis of a large variety of practical waveguides and lasers, allowing for many layers and material loss and gain [9]. Moreover, the FSRM method has been used to calculate the facet reflectivity of 1D and 2D waveguides with high accuracy [10,11]. The FSRM method assumes that the refractive index difference between core and cladding is small, typically less than 10 %, and then assumes that the radiation modes propagate through a medium of uniform refractive index.

The increasing need to couple general optoelectronic circuits to fibres requires that waveguides buried at realistic depth from the air-semiconductor boundary are also considered. In such cases the air-semiconductor boundary makes a strong impact on the fields in the waveguide, as well as on the facet reflectivity, and can not be neglected.

A novel Half Space Radiation Mode (HSRM) method has been developed for the analysis of shallowly buried waveguides. It has been shown that propagation constant and the modal field profiles can be significantly affected by the presence of the air-boundary [12]. The HSRM method has also been extended to calculate the facet reflectivity of shallowly buried waveguide structures. Low facet reflectivity is important for the proper operating of optical amplifiers and when coupling between the guides is required. In the case of shallowly buried waveguides, it is expected that the air- semiconductor boundary and 3D-corner (Fig. 2) will cause increased modal reflectivity. Results for facet reflectivity of a 1D waveguide normally incident on an antireflection (AR) coated facet show that the presence of the air-semiconductor boundary and facet corner can not be neglected. Typically, a semiconductor amplifier structure with two AR coatings, designed for -40 dB reflectivity for both TE and TM polarisation, can show an increase in reflectivity of up to 10 dB when the waveguide is in the vicinity of an air boundary [13].

In this paper we will present our latest results from further recent development of the SI and HSRM methods. The SI method has been extended

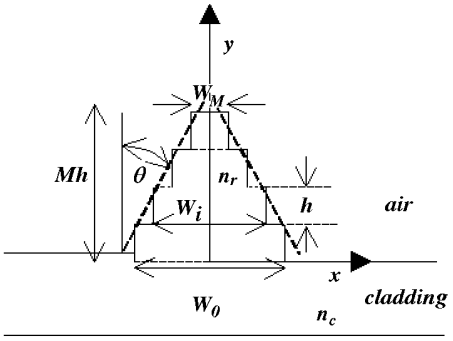

Fig. 1. Modelling oblique rib waveguide with M sections of constant height h.

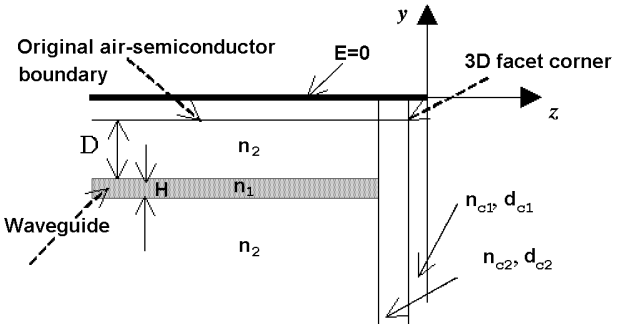

Fig. 2. Side view of a waveguide incident on the facet plane.

to include the practical case of imperfect walls (e.g. the schematic non-rectangular cross- section shown in Fig. 1 which arise from certain manufacture processes, both intentionally and unintentionally). Also the extension of the HSRM method to account for the effect of the air-semiconductor boundary and a 3D facet corner (Fig. 2) will be described. Both methods will be described in detail for the case of TE polarisation only. The analysis for the TM polarisation follows similarly.

2. SI Method for Imperfect Rib Geometries

Since the original development of the SI method when it was used to solve for the propagation constant of the air-clad rib waveguides, the SI method has been enhanced to include field singularities at the re-entrant rib corners [7], identify the radiation spectrum, and has also been applied to vertical rib couplers and 3D propagation problems. Here we focus on

the extension of the SI method to arbitrarily shaped rib geometries with an air cladding. The versatility of the method primarily lies in its simplicity of formulation and ease of implementation. For the simplest case of a rib guide with guide and cladding layers, the method proceeds in 3 phases: a) application of the concept of effective widths by which the field penetration into the air cladding is modelled [6], b) description of the field in the rib in terms of a Fourier series and the field in the cladding as a superposition of plane waves and c) formulation of a transcendental equation for β by applying the variational boundary condition to match the field derivative at the base of the rib. The method is very efficient and accurate, producing results in a matter of seconds.

Consider the general case of arbitrary shaped rib waveguide. The rib is split into M sections of constant height h and variable width W_i as shown in Fig. 1. The idea of the method is to establish the connection between the field at the base of the rib and the field at the top of the rib. A transcendental equation for the propagation constant β is obtained by enforcing two conditions: a) the condition that $E = 0$ at the top of the rib ($y = M_h$), and b) the continuity of the fields at the base of the rib ($y = 0$).

The field and its derivative at the base of the rib ($y = 0$) can be in general case expressed as

$$\begin{aligned} E(x,0) &= \sum_{i=1}^{N} V_{0i}\Big[\sqrt{\frac{2}{W_0}}\cos(\frac{n\pi x}{2W_0})\Big] \\ \frac{\partial E(x,0)}{\partial y} &= \sum_{i=1}^{N} I_{0i}\Big[\sqrt{\frac{2}{W_0}}\cos(\frac{n\pi x}{2W_0})\Big] \end{aligned} \tag{1}$$

or in matrix form as

$$\begin{bmatrix} E(x,0) \\ \dfrac{\partial E(x,0)}{\partial y} \end{bmatrix} = \begin{bmatrix} \overline{F}_0^T & 0 \\ 0 & \overline{F}_0^T \end{bmatrix} \begin{bmatrix} \overline{V}_0 \\ \overline{I}_0 \end{bmatrix} \tag{2}$$

where N is the number of terms, the overbar symbol '$\overline{\ }$' indicates submatrices and 'T' indicates the transpose matrix. The field and derivative at the next discontinuity ($y = h$) can be expressed using ABCD matrix notation, i.e.,

$$\begin{aligned} \begin{bmatrix} E(x,0) \\ \dfrac{\partial E(x,0)}{\partial y} \end{bmatrix} &= \begin{bmatrix} \overline{F}_0^T & 0 \\ 0 & \overline{F}_0^T \end{bmatrix} \begin{bmatrix} \overline{A}_0 & \overline{B}_0 \\ \overline{C}_0 & \overline{D}_0 \end{bmatrix} \begin{bmatrix} \overline{V}_0 \\ \overline{I}_0 \end{bmatrix} \\ &= \begin{bmatrix} \overline{F}_0^T & 0 \\ 0 & \overline{F}_0^T \end{bmatrix} \begin{bmatrix} \overline{T}_{01}^T & 0 \\ 0 & \overline{T}_{01}^T \end{bmatrix} \begin{bmatrix} \overline{A}_0 & \overline{B}_0 \\ \overline{C}_0 & \overline{D}_0 \end{bmatrix} \begin{bmatrix} \overline{V}_0 \\ \overline{I}_0 \end{bmatrix} \end{aligned} \tag{2}$$

where $\overline{A}_0$, $\overline{B}_0$, $\overline{C}_0$, $\overline{D}_0$ are diagonal submatrices with elements $A_{0mn} = D_{0mn} = \cos(\gamma_r h)$, $B_{0mn} = \gamma_r \sin(\gamma_r h)$, $C_{0mn} = -\sin(\gamma_r h)/\gamma_r$, $n = 1, 2, \ldots, N$ with $\gamma_r = \sqrt{(k_0 n_r)^2 - s^2 - \beta^2}$, where n_r is the rib refractive index. The submatrix $\overline{T}_{01}$ is of order $N \times N$ and defines the overlapping of the fields in the successive rib sections, with elements as

$$(T_{01})_{i,j} = \int_0^{W_1} dx F_{0i} F_{0j}, \quad i, j = 1, \ldots, N$$

Proceeding in the similar manner towards the top end of the rib, we get

$$\begin{bmatrix} E(x, Mh) \\ \dfrac{\partial E(x, Mh)}{\partial y} \end{bmatrix} = \begin{bmatrix} \overline{F}_M^T & 0 \\ 0 & \overline{F}_M^T \end{bmatrix} \begin{bmatrix} \overline{\alpha} & \overline{\beta} \\ \overline{\gamma} & \overline{\delta} \end{bmatrix} \begin{bmatrix} \overline{V}_0 \\ \overline{I}_0 \end{bmatrix} \tag{4}$$

Below the base of the rib it is suitable to define

$$\overline{I}_0 = \overline{Y V_0} \tag{5}$$

where

$$Y_{ij} = \int_0^{\infty} ds F_{0i}(s) F_{0j}(s) \Gamma(s).$$

$F_{0i,j}(s)$ are Fourier transforms of elements of the submatrix F_0 and $\Gamma(s)$ is the plane wave response of the multilayered substrate.

Enforcing the condition $E(x, Mh) = 0$ and substituting (5) into (4) transcendental equation for β is obtained in the form

$$|\overline{\alpha} + \overline{\beta Y}| = 0. \tag{6}$$

3. HSRM Method for 2D Facet Analysis

The HSRM method deals with the guided mode(s) exactly but approximates the radiation modes by assuming that they propagate through a medium of uniform refractive index (n_{un}). The penetration of the optical field into the air is modelled by moving the original air-semiconductor boundary to a new one on which the condition $E = 0$ is set. Thus the fields are present only in the half space, hence the name of the method.

Looking at the structure shown in Fig. 2 it can be seen that the field in the waveguide ($z < 0$) is restricted to the half space ($y < 0$), whereas the field outside the facet ($z > 0$) is unlimited in the y direction. The HSRM method solves the problem in Fourier space and applying the 2D

Fourier transform on the field in the waveguide will involve convolution, which will significantly degrade the efficiency of the method. In order to avoid convolution, the 2D Fourier transform is chosen such that along y direction the Fourier Sine transform (FST) is applied for the fields inside the waveguide and the exponential Fourier transform (FT) for the fields outside the facet. Along the x-direction the exponential Fourier transform is applied in both regions. Hence, the electric and magnetic field in the waveguide are

$$e^{-}(p,s) = e_i(p,s) + Re_r(p,s) + r(p,s), \quad z < 0 \tag{7}$$

$$h^{-}(p,s) = h_i(p,s) + Rh_r(p,s) + Y_r r(p,s). \quad z < 0 \tag{8}$$

and outside the facet

$$e^{+}(p,t) = f(p,t), \quad z > 0 \tag{9}$$

$$h^{+}(p,t) = Y_f f(p,t), \quad z > 0 \tag{10}$$

where p is x-directed Fourier variable and s and t are y-directed Fourier variables which are in general different.

The field in the guide is comprised of incident (e_i) and reflected (e_r) guided modes and the backward scattered radiation spectrum (r). R is the modal reflection coefficient. The field outside the facet is represented as a plane wave spectrum (f). Y_r and Y_f are admittances, which for the TE polarisation are

$$Y_r = -\frac{\gamma_r^2 + p^2}{\gamma_r}, \quad Y_f = \frac{\gamma_f^2 + p^2}{\gamma_f},$$

with $\gamma_r = (n_{un}k_0)^2 - p^2 - s^2$, $\gamma_f = (k_0)^2 - p^2 - s^2$.

The aim is to solve eq.(7-10) for the modal reflection coefficient R. This is done by enforcing the continuity of the electric and magnetic fileds at the facet plane ($z = 0$), and by imposing the required orthogonality condition between the radiation and guided modes of the form

$$\int_0^\infty ds \int_{-\infty}^{\infty} dp r(p,s) h_r(p,s) = 0.$$

However, simply equating eqs.(7) and (9), and eqs.(8) and (10) is not possible due to the different spectral variables. To get around this problem, we have developed an iterative procedure which starts by estimating a starting value for the reflection coefficient $R^{(0)}$. $R^{(0)}$ is found by solving eq.(7-10)

for a modified structure in which air-semiconductor boundary is extended along whole z-range. Thus the spectral variables in both regions ($z < 0$, and $z > 0$) are the same and $R^{(0)}$ can be straightforwardly found as

$$R^{(0)} = \frac{\int_0^\infty ds \int_{-\infty}^{\infty} dp \frac{Y_f(p,s)e_i(p,s) - h_i(p,s)}{Y_f(p,s) - Y_r(p,s)} h_r(p,s)}{\int_0^\infty ds \int_{-\infty}^{\infty} dp \frac{h_r(p,s) - Y_f(p,s)e_r(p,s)}{Y_f(p,s) - Y_r(p,s)} h_r(p,s)} \tag{11}$$

An iterative procedure in which the magnetic field $h(p,t)$ is reexpressed in terms of p and s variables is then adopted as follows:

$$\begin{aligned} f(p,s) \overset{IFST}{\rightarrow} f(x,y) \overset{FFT}{\rightarrow} f(p,t) \overset{Y_A(p,t)}{\rightarrow} h(p,t) \\ \overset{IFFT}{\rightarrow} h(x,y) \overset{FST}{\rightarrow} h(p,s) \rightarrow R(eq.13) \end{aligned} \tag{12}$$

The reflection coefficient was obtained using

$$R = \frac{\int_0^\infty ds \int_{-\infty}^{\infty} dp \frac{h(p,s) - h_i(p,s)}{Y_r(p,s)} h_r(p,s)}{\int_0^\infty ds \int_{-\infty}^{\infty} dp \frac{h_r(p,s)}{Y_r(p,s)} h_r(p,s)} \tag{12}$$

The iterative procedure eq.(12) is repeated until convergence on R is achieved, which in most cases requires no more than 4-5 iterations. The method is very fast producing results in a couple of minutes.

4. Results

4.1 SI method

The rib waveguide structure shown in Fig. 1 is analysed. The rib width at the base of the rib is $W_0 = 3\ \mu m$ and the operating wavelength is $\lambda = 1.15\ \mu m$. Fig. 3 shows the dependence of the normalised propagation constant b versus rib height, for different rib wall slopes. It can be seen that for small rib heights, the shape of the rib does not influence the propagation constant, due to the fact that most of the field is concentrated in the region below the rib. However, for the larger rib heights, the rib shape can significantly influence the propagation constant and hence the field pattern.

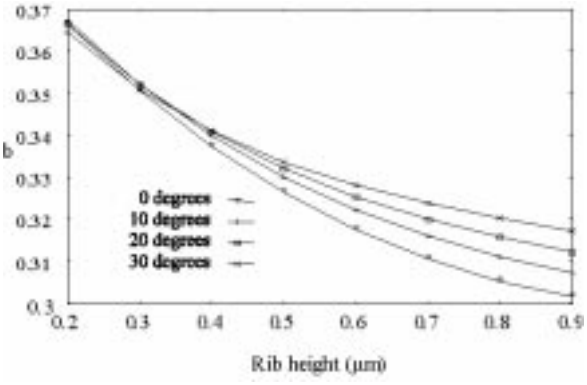

Fig. 3. The dependence of the propagation constant b on the rib height for different rib wall slopes.

4.2 HSRM method

Very low facet reflectivity ($< 10^{-4}$) is required for the correct operation of semiconductor optical amplifiers. One of the techniques for reducing facet reflectivity is to place antireflection coatings (AR) at the end of the facet. The first structure analysed corresponds to a semiconductor amplifier with core and cladding refractive indices of $n_1 = 3.52$ and $n_2 = 3.2$ respectively. The waveguide has width $W = 1.5\ \mu m$ and height $H = 0.15\ \mu m$ and the operating wavelength is $\lambda = 1.3\ \mu m$. The facet is coated with one AR coating. Two cases are considered; with the waveguide (1) deeply buried in the substrate, $(D \to \infty)$, and (2) buried at a depth $D = 1\ \mu m$. Fig. 4 shows contours of equal reflectivity for the TE polarized mode supported by the waveguide. Contours of equal reflectivities of -30 and -40 dB are plotted against the refractive index of the coating and its normalised thickness (d_c/λ_c), where d_c is the coating thickness and λ_c is the wavelength in the coating. It can be seen that in order to maintain low reflectivity the amplifier structure has to have different coating parameters for the two waveguide geometries.

The second structure has waveguide dimensions $W = 1\ \mu m$ and $H = 0.2\ \mu m$ and refractive indices $n_1 = 3.517$, $n_2 = 3.17$. The facet is coated with two AR coatings with parameters $n_{c1} = 1.4431$, $d_{c1} = 0.3183\ \mu m$, $n_{c2} = 2.5161$ and $d_{c2} = 0.1783\ \mu m$. Fig. 5 shows the power reflectivity versus wavelength for different buried depths D for both TE and TM polarisations. It can be seen that with decreasing buried depth D, power reflectivity increases above the acceptable level (10^{-4}). Thus, when using shallowly buried guides the AR coating needs to be redesigned.

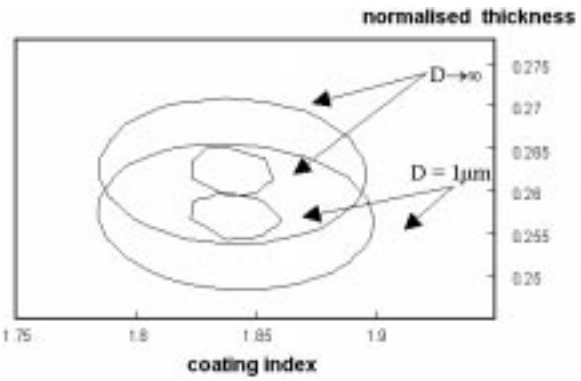

Fig. 4. The variation of TE mode reflectivity using a single layer AR coating for the depth $D = 1\ \mu m$ and $D \to \infty$.

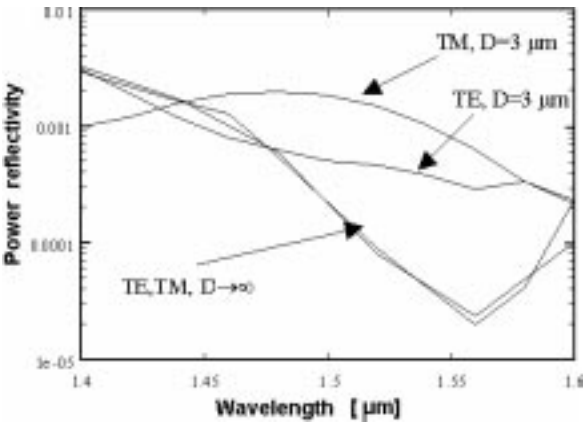

Fig. 5. Power reflectivity versus wavelength for buried depths $D = 3\ \mu m$ and $D \to \infty$, for both TE and TM polarisations.

5. Conclusions

The SI method has been extended to include the case of arbitrary shaped rib geometries. It has been shown that for larger rib heights, the shape of the rib can significantly affect the modal propagation constant. The HSRM method has been developed to calculate facet reflectivity for shallowly buried 2D waveguides. It has been shown that in a case of optical amplifiers, small buried depth can significantly increase modal reflectivity and can therefore be detrimental for correct operating.

REFERENCES

1. M. S. Stern: *Finite Difference Analysis of Planar Optical Waveguides.* Chapter 4, PIER 10, part I, EMW publishing, 1995.
2. A. J. Davies: *The Finite Element Method: A First Approach.* Oxford University Press, 1980.
3. W. P. Huang, C. L. Xu: *Simulation of three dimensional optical waveguides by a full vector beam propagation method.* IEEE J. Quantum Electron. vol. 29, No.10, 1993, pp. 2639-2649.
4. R. M. Knox, P. P. Toulies: *Integrated circuits for the millimetre through optical frequency range.* Proc. M. R. I. Symp. Submillimetre waves, Fox J., Ed. Brookin, N. Y.: Polytechnic Press, 1970, pp. 497-516.
5. P. C. Kendall, M. J. Adams, S. Ritchie, M. J. Robertson: *Theory for calculating approximate values for the propagation constants of an optical rib waveguide by weighting the refractive indices.* IEE Proc. A, vol. 134, 1987, pp. 699-702.
6. P. C. Kendall, P. McIlroy, M. S. Stern: *Spectral index method for rib waveguide analysis.* Electron. Lett., vol. 25, 1989, pp. 107-108.
7. A. Vukovic, P, Sewell, T. M. Benson, P. C. Kendall: *Singularity-corrected spectral index method.* IEE Proc. Optoelectronics, vol. 145, No.1, 1998, pp. 59-64.
8. M. Reed, T. M. Benson, P. Sewell, P. C. Kendall, G. M. Berry, S. V. Dewar: *Free Space Radiation Mode analysis of rectangular waveguides.* Optical and Quantum Electronics, vol. 28, 1996, pp. 1175-1179.
9. M. Reed, P. Sewell, T. M. Benson, P. C. Kendall, M. Noureddine: *Computationally efficient analysis of buried rectangular and rib waveguides with applications to semiconductor lasers.* IEE Proc.-Optoelectron., vol. 144, 1997, pp. 14-18.
10. M. Reed, T. M. Benson, P. Sewell, P. C. Kendall: *FSRM method for the analysis of coated angled facets and comparison with FD-TD results.* Microwave and Optical Tech. Letters, vol. 15, No.1, 1997, pp. 12-16.
11. P. Sewell, M. Reed, T. M. Benson, P. C. Kendall: *Full vector analysis of two-dimensional angled and coated optical waveguide facets.* IEEE J. of Quantum Electron., vol. 33, 1997, pp. 2311-2317.
12. A. Vukovic, P. Sewell, T. M. Benson, P. C. Kendall: *Novel half space radiation mode method for buried waveguide analysis.* Optical and Quantum Electronics, vol. 31, 1999, pp.43-51.
13. A.Vukovic, P. Sewell, T. M. Benson, P. C. Kendall: *Degraded facet performance caused by edge proximity.* Electronics Letters, vol. 34, 1998, pp. 1939-1940.